Nanotechnology Perceptions
ISSN 1660-6795
www.nano-ntp.com

Comprehensive Analysis of Structural, Electronic, Thermodynamic and Thermoelectric Properties of Fe_2SnSe_4

Hadjer Dilmi[1,2], Sabah Fetah[1,2*], Abdelouahab Bentabet[3]

[1]Department of Physics, Faculty of science. University of M'sila, Algeria
[2]Laboratory of materials and renewable energy, Faculty of science, University of M'sila, Algeria
[3]Institute of sciences and technologies, University of Bordj Bou Arreridj, Algeria
Email: sabah.fetah@univ-msila.dz
Received: 12/12/2023, Revised: 05/04/2024, Accepted: 02/07/2024, Published: 26/09/2024

Abstract: Functional density theory within the framework of the FP-LAPW method based on the generalized gradient approximations, GGA(WC, PBE, PBEsol) and GGA(WC, PBE, PBEsol) +U, were used to compute the exchange-correlation potential in order to examine the crystal structure, electronic structure, density of states, and magnetic properties of Fe_2SnSe_4 compound characterized by its orthorhombic olivine-type structure and classified under space group Pnma

The calculations indicate that the Fe_2SnSe_4 compound maintains stability within the ferromagnetic configuration. The GGA(WC, PBE, PBEsol) approximations provide a more accurate description of semiconductor behavior, revealing the presence of a direct band gap. Nonetheless, the (GGA-PBEsol+U) approximation demonstrates remarkable agreement, proving to be both significant and effective in forecasting the magnetic moments of the examined compound, while also yielding a lattice constant that is very close to the experimental value. In this approach, the significant Coulomb repulsion between localized d states of Fe is addressed by incorporating a Hubbard U parameter into the standard (GGA) approximations.

The study focuses on examining the stability of the material and analyzing its thermoelectric performance. The thermodynamic parameters of the compound Fe_2SnSe_4 are calculated, with particular attention given to volume and compressibility modulus, specific heats at constant volume and constant pressure , Debye temperature , and entropy. Furthermore, the thermoelectric parameters such as Seebeck coefficients, electrical conductivity, thermal conductivity, and power factor are determined as functions

of temperature. The computational results indicate that the Fe_2SnSe_4 material shows significant promise for thermoelectric applications

Keywords: Density Functional Theory (DFT) ,GGA, GGA+U, structural stability, Transport properties.

1. Introduction

The magnetic and thermoelectric properties of ternary chalcogenide semiconductors (II=Mn, Fe, Co; IV=Si, Ge, Sn; VI=S, Se, Te) have garnered significant interest. The interaction between electron spins, facilitated by the coexistence of transition metal and chalcogenide elements within the same molecule, leads to potential applications. These substances are ternary chalcogenides that crystallize in the olivine-type structure and belong to the adamantine family. Recent studies indicate that the Olivine iron-atom-containing ternary chalcogenides Fe_2GeS_4 and Fe_2SiS_4 [7] exhibit a stable phase. The materials exhibit higher absorption coefficients and proposed band gaps of 1.40 eV and 1.55 eV, respectively, indicating their enhanced suitability for solar light absorption. The characteristics of these two materials render them suitable for photovoltaic applications. Olivine compounds containing Fe with Se and Te anions demonstrate significant thermoelectric performance. The physical characteristics of Fe_2SnSe_4 were studied using powder X-ray diffraction techniques [4]. Quintero et al. [12] documented the ferromagnetic behavior of Fe_2SnSe_4, representing one of the limited publications on this topic.

However, no comprehensive study has been reported, and only limited crystallographic information is available. The crystal structure of the ternary magnetic compound Fe_2SnSe_4 was refined via powder X-ray diffraction employing the Rietveld method. The material was synthesized using the melt and annealing technique, resulting in crystallization with an olivine structure within the orthorhombic space group Pnma.[4]. This compound belongs to the II2-IV-VI4 family of semiconductors and features an olivine-type structure. The structural characterization of the sample reveals that Fe_2SnSe_4 exhibits an orthorhombic olivine-type structure, belonging to space group Pnma. The unit cell parameters are a = 13.2019(3) Å,

b = 7.6746(1) Å, c = 6.3572(1) Å, and the volume is V = 644.11(2) $Å^3$.

This report seeks to elucidate the fundamental characteristics of Fe_2SnSe_4 by examining its properties. To date, no ab-initio studies have been conducted on the electronic, magnetic, thermodynamic, and thermoelectric properties of Fe_2SnSe_4.

2. Computational details

The density functional theory (DFT) as applied in the Vienna package Wien2k serves as the foundation for the full-potential linearized augmented plane wave (FP-LAPW) approach, which is the basis of the current ab-initio analysis. [2,8,11,14]. A multiple versions of (GGA) and (GGA+U) approximations of the generalized gradient approximation were used to treat the exchange-correlation effects. Additionally, The DFT+U method is employed to describe strongly correlated systems, as it consistently provides accurate results for the electronic and structural properties of these systems that involve d-electrons.

This approach divides the crystal's unit cell into non-overlapping muffin-tin (MT) spheres, with an interstitial space separating them. Within the non-overlapping spheres of the muffin- tin (MT) radius, RMT, The minimum radius of a muffin tin sphere (Rmt) for the Fe, Sn, and Se atoms is 2.44, 2.44, and 2.32 bohr, respectively. The interstitial region is defined by a cut- off radius of $R_{mt} \times k_{max}$, where k_{max} represents the maximum wave vector for plane waves, corresponding to the largest wave vector utilized in the development of eigen-functions in plane waves. This value is established at $R_{mt} \times k_{max} = 8.0$. Consequently, we conducted convergence tests using a maximum wave vector of $G_{max} = 12.0$, with 270 k-points evaluated in the first irreducible Brillouin zone. The convergence criterion was established at 10^{-4} Ry for the total energies.

3. Results and discussion

3.1. Structural Properties

The ternary chalcogenide Fe_2SnSe_4 is classified within the adamantine family of quaternary chalcogenides and crystallizes in an olivine-type structure. The olivine structure Fe_2SnSe_4 exhibits an orthorhombic configuration [4] characterized by the space symmetry group Pnma (N° 62). The unit cell of Fe_2SnSe_4 contains 56 atoms, equivalent to eight unit formulas (8 Fe_2SnSe_4). The conventional unit cell comprises 32 Se anions, 16 Fe cations, and 8 Sn cations, which are situated at the Wyckoff positions. Figure1 illustrates the unit cell diagram of Fe_2SnSe_4, highlighting the octahedral and tetrahedral coordination surrounding the cations. The structure features a hexagonal close packing of Se^{-2} anions, with Fe^{+2} cations occupying half of the octahedral sites and Sn^{+4} cations occupying one-eighth of the tetrahedral sites.

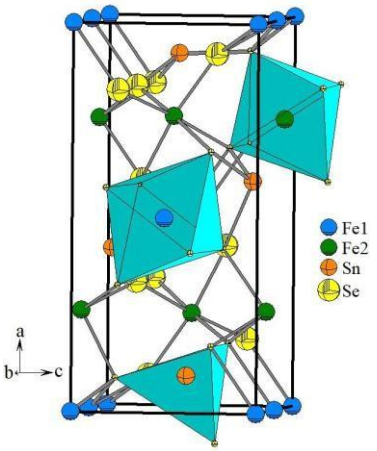

Figure 1. Unit cell diagram in the ac plane of the olivine type compound Fe_2SnSe_4 (Pnma) showing the $FeSe_6$ octahedra and $SnSe_4$ tetrahedra.

Table 1. Atomic coordinates, occupancy factors and geometric parameters (Å) for Fe_2SnSe_4

Atom	**Ox.**	**Site**	**X**	**Y**	**Z**
Fe1	+2	4a	0	0	0
Fe2	+2	4c	0.242(1)	¼	0.503(1)
Sn	+4	4c	0.407(1)	¼	0.073(1)
Se1	-2	8d	0.328(1)	0.008(1)	0.253(1)
Se2	-2	4c	0.416(2)	¼	0.688(2)
Se3	-2	4c	0.583(2)	¼	0.247(1)

The first important step in these calculations is the determination of the structural properties of Fe_2SnSe_4. Knowing this information allows us to access the electronic, magnetic, thermodynamic and thermoelectric properties. Full structural optimizations and convergence test of the considered material was performed so as to measure the stability structural parameters, together with the lattice parameters. To achieve this, some values of the lattice parameters were used and the corresponding total energy of the unit cell was calculated and the atomic positions were allowed to relax for each volume. The various values of the total energy obtained were plotted against that of volume and the resulting curve was used in fitting the Birch Murnaghan equation of state (EOS) [9] to acquire the equilibrium bulk modulus Bo, cell volume at minimum energy and the pressure derivative B_0.

The stability of ferromagnetic state of this compound has been verified by optimizing the total energy ground states according to volume for several magnetic configurations, including the paramagnetic phase (PM), ferromagnetic phase (FM), and antiferromagnetic phase (AFM). As demonstrated in figure2, the FM configuration, the spins of the Fe1 and Fe2 atoms are oriented in the same direction, however with varying amplitudes (Fe1↑, Fe2↑). In the AFM phase, the spins are aligned in parallel but orientated in opposing directions (Fe1↑, Fe2↓), leading to a net magnetic moment of zero for the material. In the PM phase , the magnetic spin moments of atoms are neglected, leading to a net magnetic moment of zero for the material.

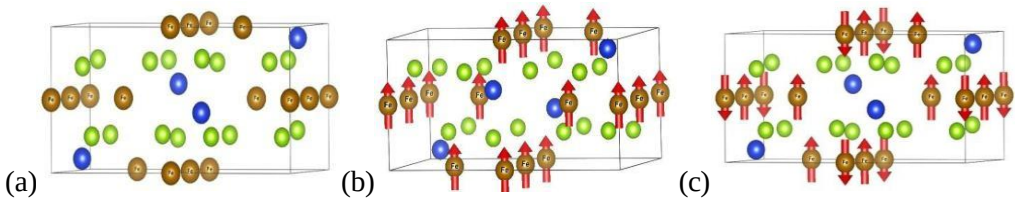

Figure 2. Schematic representation of the three magnetic configurations in the orthorhombic structure for the compound Fe_2SnSe_4 :(a) Paramagnetic (PM), (b) Ferromagnetic (FM) ,and (c) antiferromagnetic (AFM) .

In this phase, computations using the GGA potential for exchange and correlation indicate, that the most stable magnetic phase is identified as the one with the lowest energy. Consequently, the FM state is predicted to be the stable configuration, as demonstrated in Table2 and Figure 3, aligning well with the experimental results reported by Quintero et al. [12].

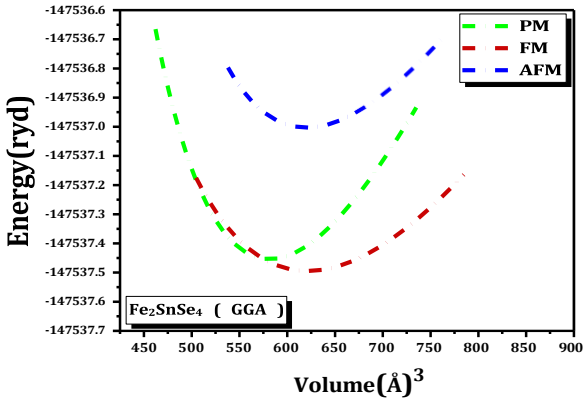

Figure 3. Volume-dependent total energy variation in the three magnetic states (FM, PM and AFM) for the compound Fe_2SnSe_4, using GGA approximation.

Table 2. Structural parameters obtained after optimization for the three magnetic configurations by using the GGA approximation for the Fe_2SnSe_4 compound, together with the available experimental result in the literature

	This work			**EXP [4]**
	PM	**FM**	**AFM**	
a(Å)	13.22	13.69	13.88	13.2
b(Å)	7.68	7.88	8.07	7.67
c(Å)	6.36	6.52	6.62	6.36
B (Gpa)	86.76	46.62	61.16	-
B'	4.92	3.35	5.00	-
V($Å^3$)	581.69	621.42	620.22	644.1
E_{min}(Ryd)	-147537.45	-147537.49	-147537.00	-
B (Gpa)	119.60	118.03	117.14	-
B'	4.24	5.00	4.59	-
V($Å^3$)	439.63	436.16	439.20	519

To further investigate the relative stability of the ferromagnetic (FM) state and in a comparative concept, several approximations have been used to treat the exchange-correlation potential: the (GGA-WC), (GGA –PBE) and (GGA-PBEsol) in our geometry optimization. Conventional GGA is known to be challenging in describing strongly correlated electrons due to the artificial delocalization of electrons. The introduction of a spurious self-interaction cannot be fully mitigated in the generalized gradient approximation (GGA), leading to an artificial delocalization of electrons. This artificial delocalization results in substantial inaccuracies in systems with highly coupled electrons. To address this issue, GGA with an additional Hubbard U parameter (GGA+U) has been used. The DFT+U method is extensively utilized for strongly correlated systems, as it reliably yields precise results for the electronic and structural properties of such systems involving d-electrons, without a substantial rise in computational expense. The strong Coulomb repulsion between localized d states of Fe is treated by adding a Hubbard-like term U = 3.9 eV, as was computed for Fe_2SiS_4 [3,5,15], to the effective potential, leading to an improved description of correlation effects.

The investigated equilibrium parameters via the different GGA and GGA+U approximations, tested in the actual work, are displayed in Table 2 and compared with the one obtained in the experimental work. One can appreciate that, there is no much discrepancy between our computed lattice parameter value and the one reported experimentally, this result indicates that our calculations are reliable. The relative deviation δ which is defined as:

$$\delta = \left(\frac{a_{cal} - a_{exp}}{a_{exp}}\right) \times 100\%$$

Where a_{cal} is the calculated lattice parameter and a_{exp} is the experimental one.

In our calculation, it is significant to note that the (GGA+ U) methods accurately predict the right shape of the unit cell we found that, δ is less than 1%. Comparing our optimized values to the experimental results, we notice that the volume values derived from approximations (GGA-WC), (GGA-PBE), and (GGA-PBEsol) are lower than the experimental results, exhibiting deviations of 3.71%, 8.54%, and 13.21% respectively. The integration of U led to a notable enhancement in the accuracy of the approximations. The (GGA-WC+U), (GGA- PBE+U), and (GGA-PBEsol+U) approximations exhibited volume overestimations of 3.67%, 5.68%, and 0.13%, respectively, when compared to experimental results. Nevertheless, the (GGA-PBEsol+U) exhibits exceptional concordance; it provides a lattice constant extremely near the experimental value.

Table 3. The Optimized lattice parameter for Fe_2SnSe_4 together with the available experimental result in the literature.

Approximations	**a(Å)**	**b(Å)**	**c(Å)**	**B(GPa)**	**B′**	**V(Å^3)**
GGA-WC	13.69	7.88	6.52	46.62	3.35	621.42
GGA-PBE	12.66	7.36	6.13	62.89	4.23	589.12
GGA-PBEsol	12.59	7.35	6.18	75.00	3.72	559.00
GGA-WC+U	13.79	8.02	6.64	66.02	4.77	667.77
GGA-PBE+U	13.43	7.65	6.47	59.91	4.97	680.73
GGA-PBEsol+U	13.21	7.68	6.36	69.33	4.49	644.94
EXP [4]	13.2	7.67	6.36			644.1

3.2. **Electronic and Magnetic properties:**

The objective of computed band structure is mainly to predict band gap energy value, which is defined as the difference between the lowest energy conduction bands of majority (minority) spin and the absolute value of the highest energy valence bands of majority (minority) potential to be used in exploring spintronic and optoelectronics application possibilities.

Structures of spin polarized electronic bands with up and down spin states are computed at the high-symmetry points within the first Brillouin zone, for the ferromagnetic Fe_2SnSe_4 compound. The band structures have been evaluated at their equilibrium lattice parameter using different approaches: GGA(WC, PBE, PBEsol) and GGA+U . For (GGA-PBE), (GGA-PBEsol) and (GGA-WC), the electronic bandgap is completely absent, as seen in Figure 4. This phenomenon is linked to the extensively reported bandgap underestimation resulting from the improper treatment of electron-exchange in standard DFT. Consequently, the Fermi energy level (zero energy point) resides within extended bands, leading to a metallic appearance of the material. In contrast, the material analyzed using (PBE + U), (PBEsol + U), and (WC + U) exhibits characteristics of a direct bandgap semiconductor, with both the valence band maximum and conduction band minimum, situated at the Γ point in the Brillouin zone. The presence of bandgap , indicating the semiconductor behavior, agree well with experimental results reported by the literature[4,12,16]. Thus, the GGA + U method offers an improved assessment of the band gap value. The computed values of the band gap (E_g) for minority- spin and the majority spin gap are given in Table 3.

This compound exhibits metallic character in both majority and minority spins, as demonstrated by calculations using the GGA (WC, PBE, PBEsol) approximations. Metallicity originates from the d states of iron (Fe) and the p states of selenium (Se) that intersect the Fermi level (E_F). When analyzed using GGA+U, this material exhibits semiconductor behavior. The density of states curves (DOS) for the Fe_2SnSe_4 compound, as illustrated in Figure 4 and figure 5, demonstrates significant similarity. The implementation of GGA does not significantly affect the form of the state density curves. The data indicate that at both band edges, Fe-3d states are predominant with a modest contribution chalcogen-p states in the valence band, as seen in figure 4. The approximation (GGA+U) reveals that the total state density displays three distinct regions in the valence band. The initial deep region ranges from [-13.40 eV to -11.76 eV], primarily characterized by the Sn^{-s} and Sn^{-p} states. The following region, spanning from [-7.24 eV to -6.67 eV], is primarily affected by the Sn^{-s} states with a lesser contribution from the Se^{-p} states. The third region, located at the upper end of the valence band within the conduction band range of [-5.93 eV, 0 eV], is mainly ascribed to Fe^{-d} states with a negligible contribution from Se^{-p} states.

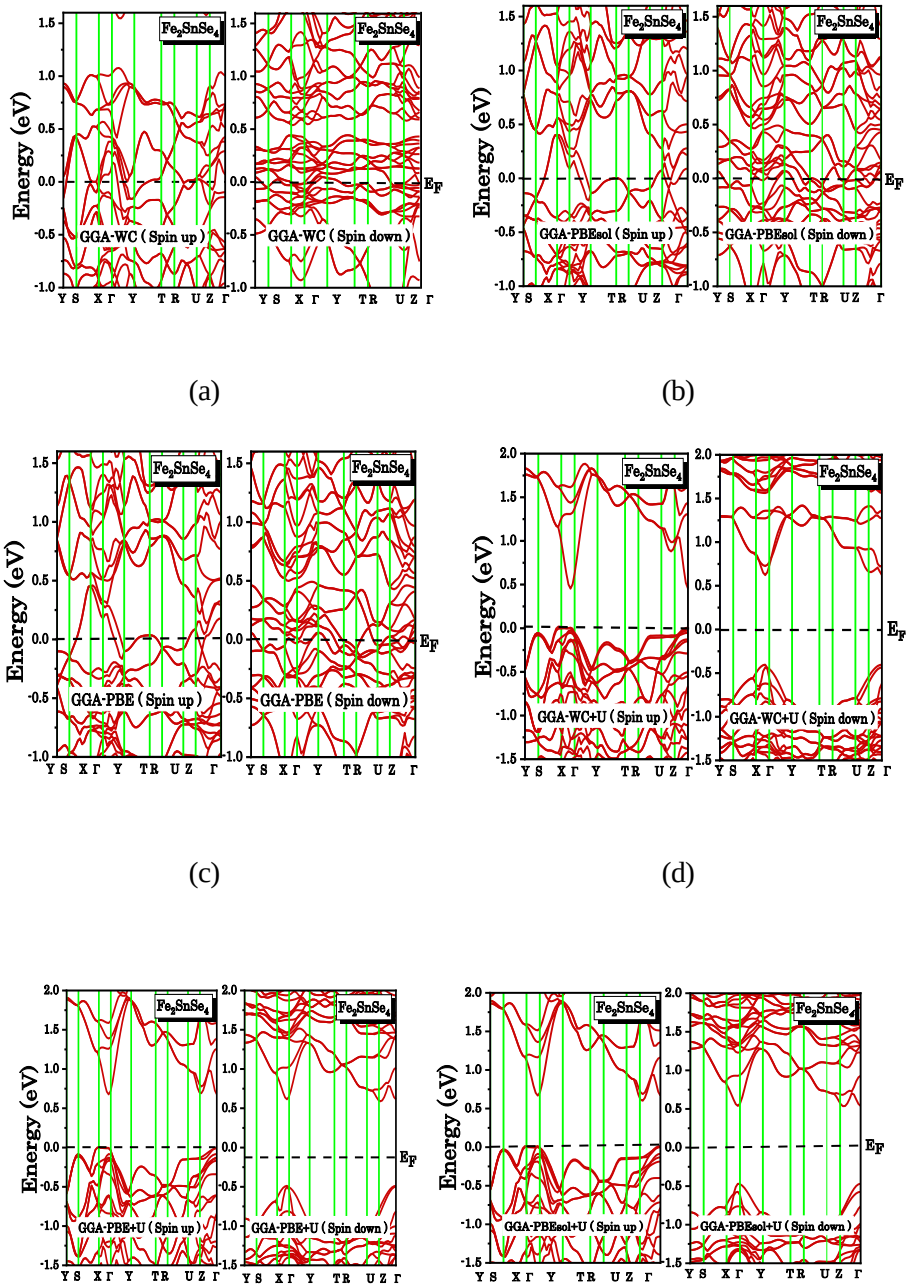

Figure.4 The Fe_2SnSe_4 Band Structure for majority spins (spin-up) and minority spins (spin-dn), using the GGA(WC,PBE, PBEsol) in (a,b,c), and using GGA(WC,PBE, PBEsol)+U in (d,e,f)

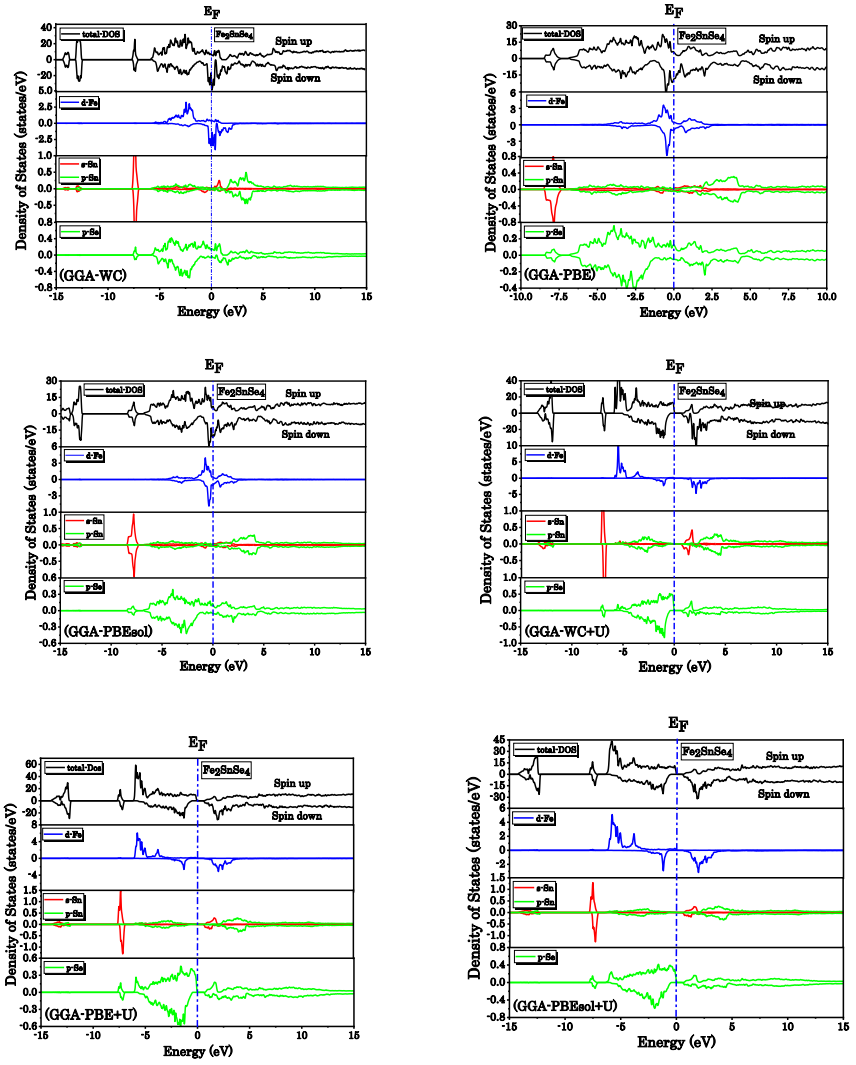

Figure5. Total and partial state density of Fe_2SnSe_4 calculated using GGA(WC,PBE, PBEsol) in (a,b,c), and using GGA(WC,PBE, PBEsol)+U in (d,e,f)

The magnetic moments of the Fe_2SnSe_4 compound were calculated using the (GGA) and (GGA+U) approximations. The results regarding the total moment of the Fe atom for various approaches and materials are presented in Table 4. The results obtained using DFT+U are higher than those from all other approaches, indicating that the introduction of the Hubbard potential effectively corrects the outcomes derived from GGA. The (GGA-PBEsol+U) exhibits exceptional concordance; as shown in the table above, it is significant and effective in predicting the magnetic moments of the studied compound and provides a lattice constant extremely near the experimental value. Consequently, we will implement this approximation for the calculation of thermodynamic and thermoelectric properties that are under consideration in this study.

Table 4. The energy gap Eg(spin↑) and Eg(spin↓) in (eV) in the majority and minority spin direction Fe_2SnSe_4 compound.

	E_g(spin ↑)	E_g (spin ↓)	μ^{Fe1}	μ^{Fe2}	$\mu^{Intertitial}$	M^{Total}
GGA-WC	Metal	Metal	2.67486	3.1089	1.16823	6.11916
GGA-PBE	Metal	Metal	0.38725	2.92394	0.47559	3.50463
GGA-PBEsol	Metal	Metal	0.44422	2.9339	0.53077	3.59258
GGA-WC+U	0.59	1.10	3.69561	3.71974	1.26345	8.00017
GGA-PBE+U	0.71	0.71	3.65411	3.68059	1.30758	8.0002
GGA-PBEsol+U	0.62	1.06	3.62787	3.65258	1.43597	8.00024

3.3. **Thermodynamic Properties**

Thermodynamic parameters of the compound Fe_2SnSe_4, are calculated. The calculations focus on volume and compressibility modulus, specific heats at constant volume (C_V) and constant pressure (C_P), Debye temperature (θ_D), and entropy across a temperature range of 0K to 1200K in increments of 100K, as well as a pressure range from 0GPa to 45GPa in increments of 5GPa.

3.3.1. Effect of temperature and pressure on volume and compressibility module

Figure 7(a) illustrates the relationship between the volume of the elemental mesh and temperature, considering various corresponding pressure values for the compound Fe_2SnSe_4.It is important to note that the same temperature change is considered for different pressures. Volume exhibits a linear increase with temperature. The rate of increase is relatively moderate across the various pressures examined. Conversely, an increase in pressure results in a decrease in volume at a constant temperature. Temperature induces an expansion of the mesh parameter which causes an increase in the volume of the material, whereas pressure results a decrease in its volume.

The compressibility coefficient quantifies a material's resistance to volume change under compression forces. The figure 7(b) illustrates the relationship between the compressibility coefficient and the variables of temperature and pressure for Fe_2SnSe_4. At constant pressure, the compressibility coefficient remains nearly constant within the temperature range of 0 K to 200 K. This can be attributed to the inadequacy of this temperature range to substantially increase the material's volume. As the temperature increases from 200K to 1200K, the compression modulus decreases resulting of the increase in the material's mesh size. Additionally, the hardness of this compound decreases with rising temperature and increases under compression.

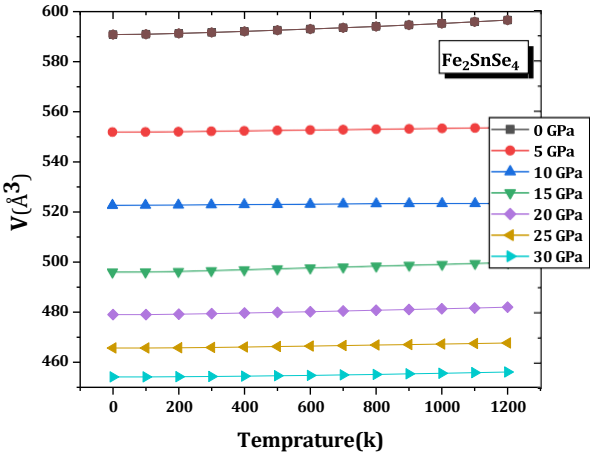

(a)

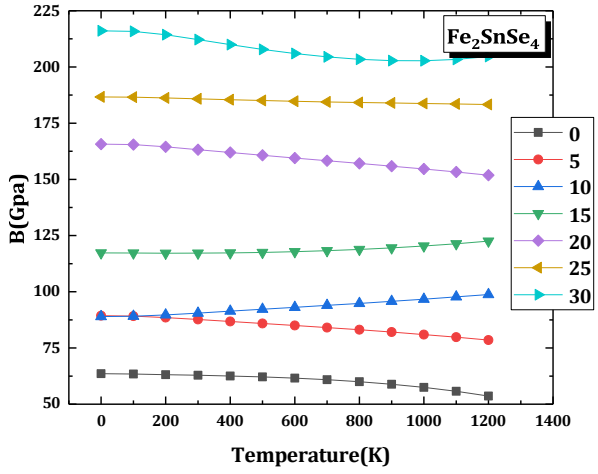

(b)

Figure 7. Temperature-dependent variation (a) ,and compressibility module variation (b) for Fe_2SnSe_4,at different pressures

3.3.2. Constant-volume heat capacity and the calorific capacity at constant pressure

The calorific capacity C_v characterizes the heat-storing ability of a material. The variation of constant volume heat capacity C_V as a function of temperature in the pressure range from 0 to 30 GPa is schematically shown on Figure 8 (a). One can distinguish two different temperature dependent behaviors in the range under consideration. At low temperatures when T< 400K, C_V increases rapidly with temperature and this is due to the anharmonic approximation of the Debye model. At high temperatures the calorific capacity slowly increases and converges towards the limit of Dulong and Petit 74.46J $mol^{-1}K^{-1}$ [6]. The calorific capacity C_v decreases by increasing pressure at a given temperature, and a value

of 65.05 $J \cdot mol^{-1} \cdot K^{-1}$ is obtained at T = 300 K and P = 0 GPa. At a constant temperature, it is observed that the calorific capacity C_v decreases with increasing pressure.The specific heat quantifies the energy or number of phonons necessary to raise the temperature of a material by one degree Kelvin. Figure 8 (b) illustrates the variation of constant pressure heat capacity C_p with temperature at various pressures for the Fe_2SnSe_4calibration. The specific heat C_p at low temperatures exhibits variations as a function of T that are analogous to those of C_v. In contrast, at elevated temperatures, C_p increases gradually and value of 69.30 $J \cdot mol^{-1} \cdot K^{-1}$ is reached at a temperature of 300 K and a pressure of 0 GPa .

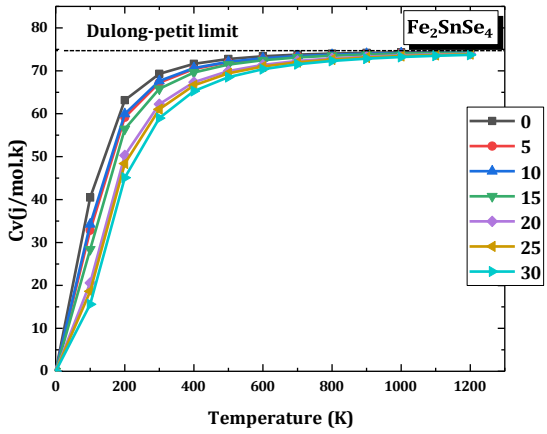

(a)

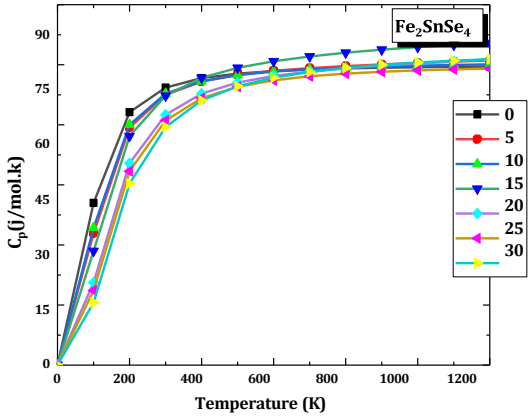

(b)

Figure 8. Variation in calorific capacity Cv (a), and the thermal capacity Cp (b) as a function of temperature for the alloy Fe_2SnSe_4 at different pressures.

3.3.3. Effect of temperature and pressure on the Debye temperature

Debye temperature [1] is a physical quantity that characterizes the behavior of the thermal capacity of solids. It is used to determine the vibrational response of a material. Figure 9 shows that the evolution of Debye temperature as a function of temperature and pressure for alloy Fe_2SnSe_4 at a fixed temperature, θ_D increases rapidly with increasing pressure and for a fixed pressure, the temperature decreases slowly with increasing temperature. At a specific temperature, the Debye temperature rises with increasing applied pressure. This behavior has been shown in the evolution of the compressibility modulus as a function of temperature and pressure. This is associated with the finding that a hard material exhibits a high Debye temperature. At 0 GPa and 300 K, the calculated value of θ_D(K) is 375K.

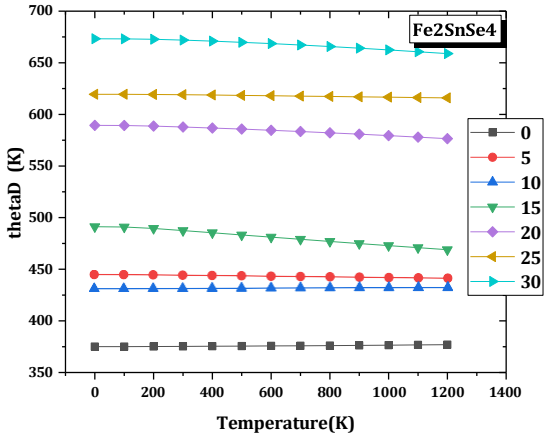

Figure 9. Variation of the temperature of Debye θD as a function of the temperature at different pressures for the compound Fe_2SnSe_4

3.3.4. Entropy (S)

Entropy is a significant thermodynamic quantity that quantifies the disorder within a system. The figure 10 illustrates the relationship between entropy (S), temperature, and pressure for Fe_2SnSe_4. It is observed that at a temperature of T = 0K, the entropy values are zero regardless of the pressure applied. At a constant pressure, entropy exhibits an exponential increase with rising temperature, while it decreases with increasing pressure at a fixed temperature. As indicated by the graph, entropy decreases with pressure, suggesting that Fe_2SnSe_4may experience a phase transition or increased rigidity when subjected to compression.

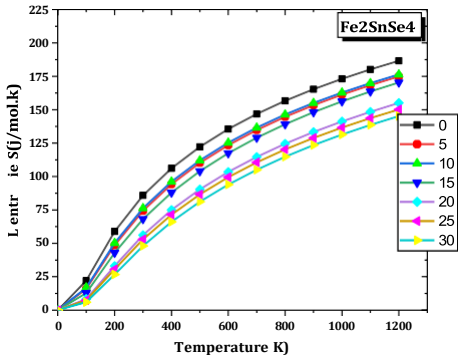

Figure.10. Variation of the entropy S as a function of temperature at different pressures for the compound Fe_2SnSe_4.

The calculated thermodynamic parameters at T = 300K and P = 0GPa , reported in Table5, offer critical insights into the structural, mechanical, and thermal properties of Fe_2SnSe_4. With a moderate bulk modulus of about 63GPa, $Fe_2SnSe_4$is not very compressible but can adjust under pressure. The Dulong-Petit law suggests that the expected high-temperature limit[6] for most solids is $Cv \approx 3R = 74.8$ J mol^{-1} K^{-1}. Fe_2SnSe_4 compound exhibits a Cv value near this limit (~65 J/mol.K), signifying nearly complete phonon excitation at 300K. The minimal difference between Cp and Cv (approximately 4.25 J mol^{-1} K^{-1}) indicates a low thermal expansion. Moreover, Fe_2SnSe_4exhibits a moderate Debye temperature (θ_D=375K), indicating moderate thermal conductivity, which is significant for thermoelectric applications. Additionally, high entropy (S=85.86 J/mol.K) contributes to low lattice thermal conductivity, thereby improving thermoelectric efficiency.

Table 5. The calculated thermodynamic parameters at T = 300K and P = 0GPa

	V	B	Cv	Cp	θ D	S
T=300K	591.09 Å³	62.863 GPa	65.05	69.30	375 k	85.86
P=0GPa			J.mol^{-1}. K^{-1}	J.mol^{-1}. K^{-1}		GPa.J/mol. K

3.4. **Thermoelectric properties**

In the following, a study of the transport properties of Fe_2SnSe_4 alloy was conducted using the BoltzTrap code.[10] implemented in the Wien2k package and following the GGAPBEsol+U approximation. The most important and representative parameters of transport properties are electrical conductivity (σ/τ), thermal conductivity (k/τ), Seebeck coefficient (S) and the merit figure (ZT). For this, good materials eligible for thermoelectric applications must have a high Seebeck coefficient, high electrical conductivity like metal and low thermal conductivity like glass, a compromise that is difficult to achieve.

3.4.1. Seebeck's coefficient

The temperature gradient between the two ends of the material creates a potential difference by Seebeck effect. The free electrons move from the highest temperature to the lowest coefficient (S) is defined in units of Volt by Kelvin [12].

In the majority spin state direction, S increases with increasing temperature to its maximum value of 222.032 μVK^{-1} at 250 K then decreases to a minimum value of approximately 181,721 μVK^{-1} at 1000 K, while in the minority spin state direction, S increases by (100 K -200K) to finally reach a value of -1865.418 μVK^{-1} at 200 and decreases when the temperature rises up to T = 500 K then stabilizes at the highest temperatures (500 K -1000K). The Seebeck coefficient for the alloy is positive in the spin up channel and in the spin down channel, meaning the presence of holes as load carriers (p-type).

Using the two-stream model, the variation in the overall Seebeck coefficient S is also computed to show the nature of the studied alloy . The currents carried by both spin up and spin down electrons are taken into account in this model to obtain the σ/τ. The following formula is used to calculate and depict the overall Seebeck coefficient [13]:

$$S = \frac{\frac{\sigma}{\tau}(\uparrow)S(\uparrow) + \frac{\sigma}{\tau}(\downarrow)S(\downarrow)}{\frac{\sigma}{\tau}(\uparrow) + \frac{\sigma}{\tau}(\downarrow)}$$

Where $\frac{\sigma}{\tau}(\uparrow)$, $\frac{\sigma}{\tau}(\downarrow)$ show the calculated electrical conductivity, and S(↑), S(↓) show the Seebeck coefficient calculated for spin up and spin down, respectively.

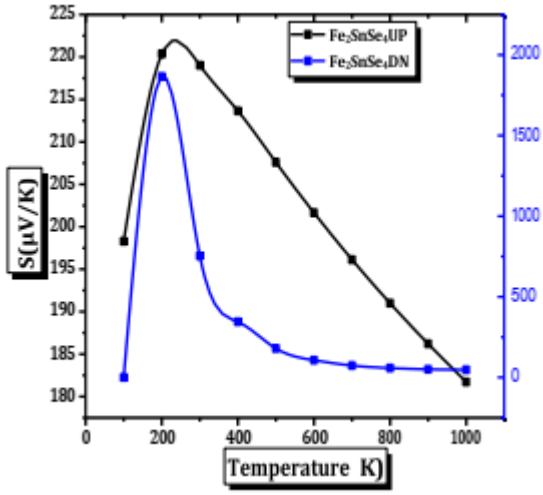

Figure.11 The variation of the Seebeck coefficient (S) and the total variation of the Seebeck coefficient (S) as a function of temperature for the compounds Fe_2SnSe_4

As clearly illustrated in Figure.11, the total Seebeck coefficient has a slightly decreasing slope. The positive sign of S explains that holes are the dominant charge carriers. Therefore, the current studied Fe_2SnSe_4 compound is p-type material. For spin-up, spin-down and spin-total channels, the Seebeck coefficient (in μV/K) calculated at ambient temperature (300K) and 0 GPa is given in Table 6.

3.4.2. Electrical conductivity:

Electrical conductivity expresses the ability of a substance or material to conduct electricity. An efficient thermoelectric material is characterized by a high electrical conductivity.

The variation of electrical conductivity with temperature for Fe_2SnSe_4, for both spin states (up and down) , is illustrated by figure 12. In the state of minority spin, σ/τ slowly increases along a quasi-linear profile with temperature, it reaches a maximum value of 2.49 10^{19} (1/Ω.cm s) for a temperature of 1000 Kc is typical behavior of semiconductors since the electrical resistivity decreases. The valence band electrons gain enough energy by increasing temperature and creating an electric current. On the other hand, for the state of minority spin σ/τ is almost constant up to 600 K, then it increases suddenly with higher temperatures and reaches a maximum value of 0.004 10^{19} (1/Ω.cm s). It is a clear indication of the semiconductor behavior of spin down states. In the two-current model, total electrical conductivity is also calculated using the following equation [12]

$$\frac{\sigma}{\tau} = \frac{\sigma}{\tau}(\uparrow) + \frac{\sigma}{\tau}(\downarrow)$$

Where $\frac{\sigma}{\tau}(\uparrow)$ and $\frac{\sigma}{\tau}(\downarrow)$ represent the total electrical conductivity for the spin up and spin down directions, respectively.

The compound Fe_2SnSe_4 has a high total electrical conductivity, which means its low electrical resistivity. Therefore, the transport of electrical charges in this material is achieved with very low heat losses (Joule effect). This implies that Fe_2SnSe_4 may be a good thermoelectric material. At ambient temperature, the electrical conductivity (σ/τ) values of Fe_2SnSe_4 alloy in spin-up, spin-down and spin-total states are reported in Table 6

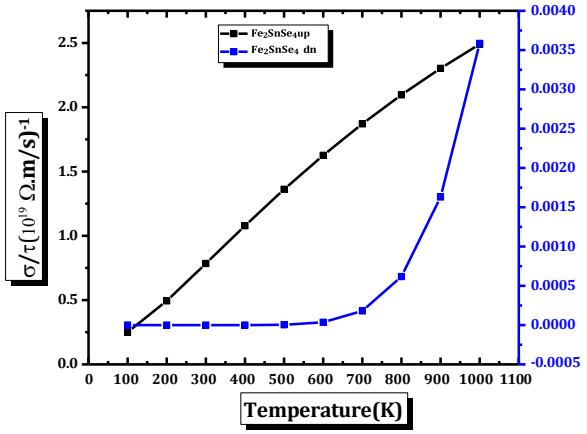

Figure 12. Total electrical conductivity (σ/τ) variation as a function of temperature for Fe_2SnSe_4 compounds

3.4.3. Thermal conductivity

Thermoelectric materials are also dependent on an extremely interesting quantity called the thermal conductivity K, which translates the transfer of energy in the form of heat resulting from a temperature change in a solid body. Thermal conductivity is the sum of the contribution of electrons and network vibrations such as $K = K_e + K_l$, where K_e and K_l are respectively

the electronic part (electrons and holes carrying heat) and the vibration part of the network (phonon contribution), with the understanding that each of these has a different temperature dependence. Thermal conductivity is influenced mainly by the network structure at ambient temperature [13]. In this study, only the electronic contribution of thermal conductivity is estimated, because the BoltzTraP code can only calculate the electronic part (Ke). The variation of this physical quantity by relaxation time as a function of temperature (Ke/τ) for both spin channels is shown in Figure13. It can be clearly observed in the state of majority spins, thermal conductivity (Ke/τ) increases linearly by 0.13 10^{14}W .m $^{-1}$. K^{-1}. S^{-1}to 100K at 11.24 10^{14} W . m^{-1}. K $^{-1}$ s $^{-1}$ to 1000 K. While for the state of minority spins, the thermal conductivity is constant up to a certain temperature threshold 600 K then grows in a non-linear way with higher temperatures to reach 0.18 10^{14} W . m^{-1}. K $^{-1}$ s $^{-1}$ to 1000 K.

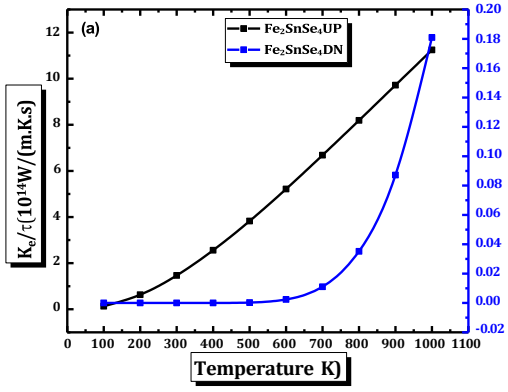

Figure 13. Temperature dependent change in electronic thermal conductivity (κ e/τ) for the compound Fe_2SnSe_4

The total electron thermal conductivity of this compound is also calculated using the expression of the two-stream model as follows [13]:

$$k_e = k_e(\uparrow) + k_e(\downarrow)$$

Where κ_e (↑) et κ_e (↓) is spin up and spin down, respectively. It exhibits a linear increase pattern as the temperature rises. Additionally, the material exhibits a low value of the total κe/τ at room temperature, which is favorable and may make it an attractive candidate for thermoelectricity. At room temperature, the values of the electronic thermal conductivity (κ e/τ) of the alloy Fe_2SnSe_4, in the spin-up, spin-down and total spin states are shown in table 6.

The merit factor (ZT) serves as an indicator of the performance of thermoelectric materials, reflecting their efficiency in generating thermoelectric energy. Materials exhibiting a ZT value of one or higher are suitable candidates for thermoelectric applications. Figure 14 illustrates the variations of this factor as a function of temperature for both spin directions. This factor indicates the performance of a thermoelectric material and its capacity to efficiently generate thermoelectric energy. ZT is determined using the following formula:

$$ZT = \frac{S^2.\sigma.T}{K}$$

Where S is the Seebeck coefficient, σ is the electrical conductivity and K is the thermal conductivity.

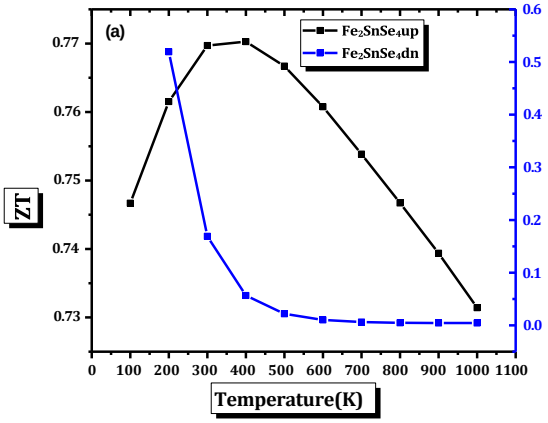

Figure14. Variation of the ZT merit factor as a function of temperature for the Fe_2SnSe_4 compound

The merit factor exhibits distinct trends between the majority and minority spin states of the Fe_2SnSe_4 compound. In the majority spin direction, the ZT increases almost linearly, reaching a maximum value of 0.770 at 400 K, followed by a decline to approximately 0.731 at 1000 K. Conversely, in the minority spin direction, a gradual decrease is noted in the temperature range of 200 K to 400 K, going from 0.519 to 0.057, after which it stabilizes and remains nearly constant at higher temperatures, above 600 K. Therefore, Spin-Up (0.78×10^{19} 1/Ω.cm.s) predominates the overall conductivity, but Spin-Down (9.49×10^{9} 1/Ω.cm.s) is significantly lower, indicating that minority spin electrons contribute minimally to the electrical current. Fe_2SnSe_4 demonstrates high electrical conductivity, particularly in the spin-up channel, which is advantageous for thermoelectric efficiency.Moreover, Spin-Up (1.74×10^{14} $W.m^{-1}.K^{-1}.s^{-1}$) is dominant in thermal conduction, but Spin-Down (9.57×10^{6} $W.m^{-1}.K^{-1}.s^{-1}$) has a negligible impact on thermal conductivity. Fe_2SnSe_4 is a promising thermoelectric material because of its low down-spin contribution, which lowers total heat conductivity and raises the thermoelectric figure of merit (ZT~1).

Table 6. Seebeck coefficient, Electrical conductivity (σ/τ) , thermal conductivity (κ e/τ) and Merit factor (ZT) at 300 K and 0GPa for the alloy Fe_2SnSe_4 in the spin-up, spin-down and spin-total states.

Etat de spin	**Up**	**Down**	**Total**
(S)[μV/K]	219.023	753.386	219.023
(σ/τ)[1/Ω·cm s]	0.78×10^{19}	9.49×10^{9}	0.784×10^{19}
(κ e/τ) [W .m $^{-1}$. K^{-1}. S^{-1}]	1.74×10^{14}	9.57×10^{6}	1.74×10^{14}
ZT	0.769	0.169	0.939

4. Conclusion:

The present study reveals that the compound Fe_2SnSe_4 exhibits stability in the ferromagnetic state configuration, which is consistent with the experimental finding . It demonstrates features of a direct bandgap semiconductor, located at the Γ point within the Brillouin zone. Furthermore, the material shows potential for low thermal conductivity, an impressive thermoelectric figure of merit (ZT=0.939) which approaches the benchmark for premium thermoelectric materials, and along with its low electronic thermal conductivity that reduces heat loss and its effective charge transport, Fe_2SnSe_4 exhibits remarkable thermoelectric properties making it a suitable candidate for thermoelectric applications. The results are entirely based on predictions, as there is a lack of experimental data.

References

1. Anderson, O. L. (1963). A simplified method for calculating the Debye temperature from elastic constants. Journal of Physics and Chemistry of Solids, 24(7), 909-917.
2. Blaha, P., Schwarz, K., Madsen, G. K., Kvasnicka, D., & Luitz, J. (2001). wien2k. An augmented plane wave+ local orbitals program for calculating crystal properties, 60(1).
3. Cococcioni, M., & De Gironcoli, S. (2005). Linear response approach to the calculation of the effective interaction parameters in the LDA+ U method. Physical Review B—Condensed Matter and Materials Physics, 71(3), 035105.
4. Delgado-Niño, P., Chacón, C., Marroquin, G., & Delgado, G. E. (2021). The chalcogenide compound Fe2SnSe4: Synthesis and crystal structure analysis by powder X-ray diffraction. Materials Research, 24(1), e20200142.
5. Dudarev, S. L., Botton, G. A., Savrasov, S. Y., Humphreys, C. J., & Sutton, A. P. (1998). Electron-energy-loss spectra and the structural stability of nickel oxide: An LSDA+ U study. Physical Review B, 57(3), 1505.
6. Fitzgerel, R. K., & Verhoek, F. H. (1960). The law of Dulong and Petit.
7. Gudelli, V. K., Kanchana, V., Vaitheeswaran, G., Singh, D. J., Svane, A., Christensen, N. E., & Mahanti, S. D. (2015). Electronic structure, transport, and phonons of SrAg C h F (C h= S, Se, Te): Bulk superlattice thermoelectrics. Physical Review B, 92(4), 045206.
8. J. P. Perdew and Y.Wang, Phys. Rev. B 45, 13244, (1992).
9. Murnaghan, F. D. (1944). The compressibility of media under extreme pressures. Proceedings of the National Academy of Sciences, 30(9), 244-247.
10. Madsen, G. K., & Singh, D. J. (2006). BoltzTraP. A code for calculating band-structure dependent quantities. Computer Physics Communications, 175(1), 67-71.
11. Perdew, J. P., Burke, K., & Ernzerhof, M. (1996). Generalized gradient approximation made simple. Physical review letters, 77(18), 3865.Perdew JP, Zunger A. Phys Rev, B 23, 5048, (1981).
12. Quintero, M., Ferrer, D., Caldera, D., Moreno, E., Quintero, E., Morocoima, M., ... & Henao, J. A. (2009). Lattice parameter values and magnetic properties for the Mn2GeTe4, Fe2GeTe4 and Fe2SnSe4 compounds. Journal of alloys and compounds, 469(1-2), 4-8.
13. Scheidemantel, T. J., Ambrosch-Draxl, C., Thonhauser, T., Badding, J. V., & Sofo, J. O. (2003). Transport coefficients from first-principles calculations. Physical Review B, 68(12), 125210.
14. Tran, F., & Blaha, P. (2009). Accurate Band Gaps of Semiconductors and Insulators with a Semilocal Exchange-Correlation Potential. Physical review letters, 102(22), 226401.
15. Yu, L., Lany, S., Kykyneshi, R., Jieratum, V., Ravichandran, R., Pelatt, B.,..... & Zunger, A. (2011). Iron chalcogenide photovoltaic absorbers. Advanced Energy Materials, 1(5), 748-753.
16. Wei, K., Martin, J., & Nolas, G. S. (2018). Synthesis and transport properties of Fe_2SnSe_4. Journal of Alloys and Compounds, 732, 218-221.